

Dynamically Tunable Scattering Manipulation of Dielectric and Conducting Cylinders Using Nanostructured Graphene Metasurfaces

*Original*

Dynamically Tunable Scattering Manipulation of Dielectric and Conducting Cylinders Using Nanostructured Graphene Metasurfaces / Hamzavi-Zarghani, Z.; Yahaghi, A.; Matekovits, L.. - In: IEEE ACCESS. - ISSN 2169-3536. - ELETTRONICO. - 7:(2019), pp. 15556-15562. [10.1109/ACCESS.2019.2894760]

*Availability:*

This version is available at: 11583/2740275 since: 2019-10-15T09:49:43Z

*Publisher:*

Institute of Electrical and Electronics Engineers Inc.

*Published*

DOI:10.1109/ACCESS.2019.2894760

*Terms of use:*

This article is made available under terms and conditions as specified in the corresponding bibliographic description in the repository

*Publisher copyright*

(Article begins on next page)

Received December 10, 2018, accepted January 17, 2019, date of publication January 24, 2019, date of current version February 12, 2019.

Digital Object Identifier 10.1109/ACCESS.2019.2894760

# Dynamically Tunable Scattering Manipulation of Dielectric and Conducting Cylinders Using Nanostructured Graphene Metasurfaces

ZAHRA HAMZAVI-ZARGHANI<sup>1,2</sup>, ALIREZA YAHAGHI<sup>1</sup>,  
AND LADISLAU MATEKOVITS<sup>ID</sup><sup>2</sup>, (Senior Member, IEEE)

<sup>1</sup>School of Electrical and Computer Engineering, Shiraz University, Shiraz 71946, Iran

<sup>2</sup>Dipartimento di Elettronica e Telecomunicazioni, Politecnico di Torino, Turin 10129, Italy

Corresponding author: Ladislau Matekovits (ladislau.matekovits@polito.it)

This work was supported in part by the Compagnia di San Paolo in the framework of the Joint Projects for the Internationalization of Research-2017 through the project Advanced Nonradiating Architectures Scattering Tenuously and Sustaining Invisible Anapoles.

**ABSTRACT** Nanostructured graphene metasurface is considered for the dynamically tunable scattering manipulation of dielectric and conducting cylinders. It is analytically shown that changing scattering width of dielectric and conducting cylinders into one of the cylinders with desired radii is possible. To achieve this purpose, the required surface impedance of the covering metasurface is derived. By properly tuning the chemical potential of the graphene, the given cylinder can controllably be seen as one with larger or smaller radii without changing the geometry of the metasurface. The simulation results of the scattering width and the 3-D far-field radar cross-section of the cylinders verify the analytical approach.

**INDEX TERMS** Graphene, metasurface, scattering, tunable.

## I. INTRODUCTION

Recently, electromagnetic cloaking which could be considered as an elegant radar cross section (RCS) reduction method has attracted significant interests [1]. Many different methods have been introduced for invisibility achievement [2]–[4]. The most known approach is transformation optics [5]–[8]. In this method, inhomogeneous and anisotropic materials cover the object in order to prevent electromagnetic waves from interacting with it. Although this technique in theory works perfectly for any objects, fabrication difficulties make its usage limited [9], [10]. Another approach is plasmonic cloaking based on scattering cancellation method. Unlike the transformation optics technique, this method allows the wave to interact with the object. For this purpose, materials with negative or near zero dielectric constant cover the object. Scattered fields of the surrounding medium and of the object cancel each other, so that the object becomes invisible [11]–[16]. In [17]–[24] another approach, which is also based on scattering cancellation method and named mantle cloaking has been proposed. Contrary to the other two methods this technique does not need volumetric medium but an ultrathin metasurface covers the object. Induced surface current at the metasurface radiates anti-phase field which cancels scattered field from the object.

With metasurfaces one can not only make an object invisible, but also in general case and by properly designing of the covering metasurface, it is possible to transform the scat-

tered signature of an object to one of another desired object. In other words, we can optimize the surface impedance associated to the metasurface to manipulate scattered field of an object and make it appears as smaller or larger or even of different shape and/or built up of different material [25]. This effect can confuse observing radars.

In [26], a formula for the required impedance of a metasurface has been derived in order to change the scattering properties of a dielectric cylinder into ones of a cylinder with different size and material. By optimizing geometry of the metasurface, scattering manipulation of a cylinder has been achieved.

On the other hand, graphene, consisting of single layer of carbon atoms, these days has attracted remarkable interests, since its surface conductivity is tuned by changing the chemical potential by adjusting the bias voltage [27]–[30]. Exploiting this unique feature, several metasurfaces based on graphene have been investigated such as: tunable anomalous reflection [31], graphene based chiral metasurface for tunable dual-band asymmetric transmission [32], optical polarization encoding [33], sensing applications based on Fano resonator [34], tunable broadband terahertz absorption [35] and tunable polarization converter [36].

In this paper, we controllably change the scattering properties of a dielectric cylinder in such a way to be identical to a dissimilar one with a different diameter (both smaller and larger examples are reported). This purpose has been

achieved merely by properly adjusting the chemical potential of the graphene, thanks to its large tunability with respect to the applied bias voltage. By changing the chemical potential of the graphene, its conductivity is changed, so we can optimize the impedance of the graphene nanopatches in a way that without changing geometry of the metasurface, the desired scattered field is obtained. Additionally, in this paper a formula for scattering manipulation of metallic cylinder is derived.

However, one can not change the scattering properties of dielectric and conducting cylinders with merely one graphene monolayer. The reason is that for scattering manipulation of the cylinders, both inductive and capacitive surface impedances are required, whereas a graphene monolayer is inductive in the whole low terahertz range [37]. Therefore, the dual inductive-capacitive nanostructured graphene metasurface presented in [38] is employed here for design of the desired cover. Moreover, it is also mechanically flexible enough to be bent around an arbitrary object [37].

The paper includes five sections. In section 2, formulation of the scattering problem of dielectric and conducting cylinders is presented. The required impedances of the metasurfaces for changing the cylinders' scattering properties to the desired ones, are introduced. In section 3, according to the results of the previous section, nanostructured graphene metasurfaces are designed for scattering manipulation of both dielectric and metallic cylinders. The analytical results are verified with full-wave simulation of the given target and coated cylinders in section 4. Conclusion of the paper are discussed in section 5.

## II. THEORETICAL FORMULATION FOR SCATTERING MANIPULATION OF DIELECTRIC AND CONDUCTING CYLINDERS

### A. SCATTERING PROBLEM OF DIELECTRIC CYLINDER

The principle of desired scattering manipulation for dielectric cylinder has been shown in Fig. 1. Here, we want to change the scattering properties of a cylinder with dielectric constant  $\epsilon$  and radius  $a_2$  (Fig. 1(a)), to the scattering properties of a cylinder with the same  $\epsilon$  but different radius  $a_1$  (Fig. 1(c)), by covering the original cylinder using properly designed metasurface (Fig. 1(b)). The considered metasurface consists of graphene nanopatches. The cylinders are exposed by a normally incident transverse magnetic (TMz) polarized plane wave. To achieve the proposed goal, the scattering problem for both the target and coated cylinders is considered, that are further equate for their total scattering widths.

Firstly, we consider the target cylinder illuminated by a TMz polarized plane wave. The incident electric field can be expressed by an infinite sum of cylindrical waves [39].

$$E_I = \hat{z} E_0 \sum_{n=-\infty}^{\infty} j^{-n} J_n(\beta_0 r) e^{jn\phi} \quad (1)$$

while the scattered field can be written as:

$$E_S = \hat{z} E_0 \sum_{n=-\infty}^{\infty} j^{-n} c_n H_n^{(2)}(\beta_0 r) e^{jn\phi} \quad (2)$$

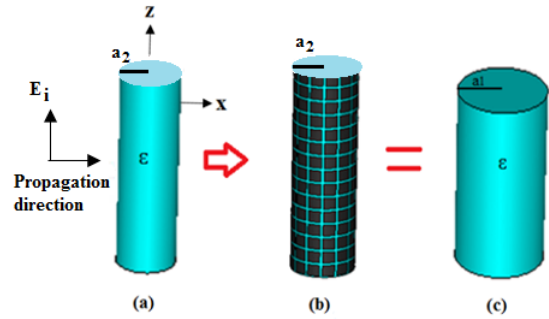


FIGURE 1. Structures of (a) given, (b) coated and (c) target dielectric cylinders.

The electric field inside the object has the expression:

$$E_{In} = \hat{z} E_0 \sum_{n=-\infty}^{\infty} j^{-n} a_n J_n(\beta r) e^{jn\phi} \quad (3)$$

where  $J_n$  and  $H_n^{(2)}$  are the Bessel function of the first kind and the Hankel function of the second kind, respectively, and  $\beta_0$  and  $\beta$  are propagation constants in free space and in dielectric medium, respectively. To obtain  $a_n$  and  $c_n$ , representing coefficients of the  $n^{th}$  harmonic, the following boundary conditions at  $r = a_1$  should be enforced:

$$E_z^1 = E_z^2 \quad (4)$$

$$H_\phi^1 = H_\phi^2 \quad (5)$$

with apex 1 and 2 corresponding to the background and to the cylinder, respectively. Electric fields for the coated cylinder have the same form as for the target cylinder but with  $a'_n$  and  $c'_n$  coefficients. Similar boundary conditions should be forced at  $r = a_2$  for the coated cylinder except eq. (5) that is replaced with the following equation:

$$Z_s (H_\phi^1 - H_\phi^2) = E_z \quad (6)$$

where  $Z_s$  is the surface impedance of the graphene nanopatches. By solving eqs. (4) and (5), coefficients of the  $n^{th}$  field expansion harmonic for the target cylinder and by solving eqs. (4) and (6), the corresponding coefficients for the coated cylinder are obtained. Their expressions are reported in eq. (7) and eq. (8), as shown at the bottom of the next page, respectively.

$$c_n = \frac{J_n(\beta a_1) J'_n(\beta_0 a_1) - \sqrt{\epsilon} J_n(\beta_0 a_1) J'_n(\beta a_1)}{\sqrt{\epsilon} J'_n(\beta a_1) H_n^{(2)}(\beta_0 a_1) - J_n(\beta a_1) H_n^{(2)'}(\beta_0 a_1)} \quad (7)$$

where  $\eta_0$  and  $\eta$  denotes the characteristic impedance of the free space (considered as background in the present investigation) and of the dielectric cylinders.

By equating total scattering widths of the target and coated cylinders, one will obtain  $\sum_{n=-\infty}^{\infty} |c_n|^2 = \sum_{n=-\infty}^{\infty} |c'_n|^2$  [26]. In [34] and [35] it has been shown that, for a cylinder with small radius in comparison to the wavelength, the first harmonic ( $n = 0$ ) is the dominant one, i.e., it has the highest contribution in total scattered field of the cylinder. So it is just needed to equate the amplitudes of the first harmonics in order to achieve the same scattered fields.

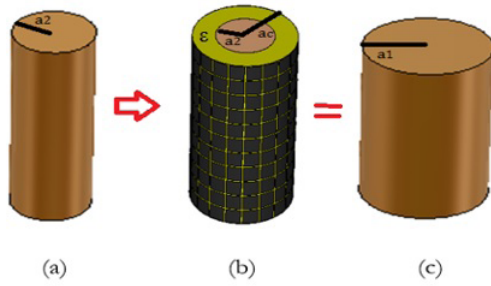


**FIGURE 2.** Structures of (a) given, (b) coated and (c) target conducting cylinders.

Using asymptotic expansion of the Bessel and Hankel functions [26], the scattering coefficients for the first harmonic are achieved as follows:

$$c_0 = j \frac{\pi(\beta_0 a_1)^2(1 - \epsilon)}{2\epsilon(\beta_0 a_1)^2 \ln(\beta_0 a_1) + 4} \quad (9)$$

$$c'_0 = \frac{\frac{4jZ_s}{\omega\mu a_2} + 4 \ln(\beta_0 a_2) + 2jZ_s \omega \epsilon_0 \epsilon a_2 \ln(\beta_0 a_2)}{\pi(\omega Z_s \epsilon_0(\epsilon - 1) - 2j)} \quad (10)$$

By equating  $c_0$  and  $c'_0$ , the result for the required impedance of the covering metasurface for achieving desired scattering manipulation of dielectric cylinder is obtained as follows:

$$Z_s = j \frac{-2\omega\mu a_2[(\beta_0 a_1)^2(\epsilon \ln(\frac{a_1}{a_2}) + \ln(\beta_0 a_2)) + 2]}{\beta_0^2(1 - \epsilon)[\epsilon a_1^2 a_2^2 \beta_0^2 \ln(\frac{a_1}{a_2}) + 2(a_2^2 - a_1^2)]} \quad (11)$$

### B. SCATTERING PROBLEM OF METALLIC CYLINDER

The principle of desired scattering manipulation for conducting cylinder is shown in Fig. 2. Fig. 2(a) represents the given conducting cylinder with radius  $a_2$ , Fig. 2(b) represents the same cylinder which has been covered by a medium with dielectric constant  $\epsilon$  and which extends up to a radius  $a_c$ . The dielectric medium is further coated by a metasurface of graphene nanopatches. The target metallic cylinder with radius  $a_1$  is shown in Fig. 2(c). Like the previous case, a TMz polarized plane wave illuminates the structure. In order to solve the scattering problem of the target cylinder, the incident and scattered fields can be written similarly to eq. (1) and eq. (2). For this case, we have only one unknown coefficient  $c_n$ , which is obtained by forcing the tangential electric field  $E_z = 0$  at  $r = a_1$ .

For the coated cylinder, the incident electric field can also be written the same as (1). The electric field inside the dielectric medium can be written as:

$$E_{In} = \hat{z} E_0 \sum_{n=-\infty}^{\infty} j^{-n} (a'_n J_n(\beta r) + b'_n Y_n(\beta r)) e^{jn\phi} \quad (12)$$

where  $J_n$  and  $Y_n$  are the Bessel functions of the first and second kind, respectively. Analogously to the previous case, the scattered field can be expressed as an infinite harmonics of

the Hankel functions of the second kind with coefficients  $c'_n$ . Due to the presence of the additional dielectric layer, that introduces a further interface, i.e., degree of freedom, in this case we have three unknown coefficients, as follows:  $a'_n, b'_n, c'_n$ . One note that the dielectric layer has the role to avoid short circuit of the graphene layer (if directly deposited on the metallic surface).

The boundary conditions, which has been proposed in eq. (4) and eq. (6) should be satisfied at  $r = a_c$ . The third equation recalls that the tangential electric field on the metal is zero, therefore we have  $E_z = 0$  at  $r = a_2$ . By solving these three equations, the scattering coefficients for the target conducting cylinder  $c_n$  and for the coated conducting cylinder  $c'_n$  are reported in eqs. (13) and (14), as shown at the bottom of the next page.

$$c_n = \frac{-J_n(\beta_0 a_1)}{H_n^{(2)}(\beta_0 a_1)} \quad (13)$$

The expression of the first harmonic for the scattering coefficients are given in eqs. (15) and (16), as shown at the bottom of the next page.

$$c_0 = \frac{-\pi}{\pi - 2j \ln(\beta_0 a_1)} \quad (15)$$

As already mentioned above, in order to achieve the same scattering properties of a thin target and coated cylinders ( $r \ll \lambda_0$ ), it is enough to equate only the first coefficients of the scattered fields from the cylinders. By equating the amplitude of  $c_0$  and  $c_0$ , we get the result for the required impedance of the metasurface reported in eq. (17), as shown at the bottom of the next page, where  $M = \sqrt{\pi^2 + 4(\ln(\beta_0 a_1))^2}$ .

### III. METASURFACE DESIGN

Nanostructured graphene metasurface is considered for controllable scattering manipulation of dielectric and conducting cylinders. The surface impedance of the planar graphene nanopatches metasurface is given by [36]:

$$Z_s = \frac{D}{\sigma_s(D - g)} - j \frac{\pi}{2\omega\epsilon_0(\frac{\epsilon+1}{2})D \ln \csc(\frac{\pi g}{2D})} \quad (18)$$

where  $D$  is the periodicity of the patches,  $g$  is the gap size between the patches,  $\epsilon$  is permittivity of the dielectric layer and  $\sigma_s$  is the surface conductivity of the graphene, which is modeled by the Kubo formula [37]. In [38], a closed form expression for the surface conductivity of the graphene, consisting of inter- and intra-band terms, has been obtained, and reported here for the sake of completeness:

$$\sigma_{intra} = -j \frac{K_B e^2 T}{\pi \hbar^2 (w - 2j\tau^{-1})} (\frac{\mu_c}{K_B T} + 2 \text{Ln}(e^{-\frac{\mu_c}{K_B T}} + 1)) \quad (19)$$

$$\sigma_{inter} = \frac{j e^2}{4\pi \hbar} \text{Ln}(\frac{2|\mu_c| - (w - j\tau^{-1})\hbar}{2|\mu_c| + (w - j\tau^{-1})\hbar}) \quad (20)$$

$$c'_n = \frac{\frac{Z_s}{j\eta_0} J_n(\beta a_2) J'_n(\beta_0 a_2) - J_n(\beta_0 a_2) (J_n(\beta a_2) + \frac{Z_s}{j\eta_0} J'_n(\beta a_2))}{-\frac{Z_s}{j\eta_0} J_n(\beta a_2) H_n^{(2)'}(\beta_0 a_2) + H_n^{(2)}(\beta_0 a_2) (J_n(\beta a_2) + \frac{Z_s}{j\eta_0} J'_n(\beta a_2))} \quad (8)$$

The overall surface conductivity of the graphene, is given by the sum of the two components, i.e., sum of  $\sigma_{intra}$  and  $\sigma_{inter}$ .

In eqs. (17) and (18),  $K_B$  is the Boltzmann's constant,  $e$  is the electron charge,  $T$  is the temperature,  $\hbar$  is the reduced Plank's constant,  $\mu_c$  is the chemical potential and  $\tau$  is the relaxation time. It can be seen that the surface conductivity of the graphene is tunable by changing frequency and  $\mu_c$ . The latter can be adjusted by changing the applied bias voltage of the graphene. This unique property makes graphene an attractive material for designing tunable and controllable devices at THz frequencies.

Here, we want to transform the scattering properties of the given dielectric cylinder with permittivity of  $\epsilon = 4$  and radius of  $a_2 = 7 \mu\text{m}$  into the target dielectric cylinders with the same material and the radii of  $a_1 = 14 \mu\text{m}$  (case  $d_1$ ) and  $a_1 = 3.5 \mu\text{m}$  (case  $d_2$ ). We want this transformation to occur at  $f = 3 \text{ THz}$  and using one metasurface but with different applied bias voltages for the graphene.

To design the desired metasurface, we should calculate the required surface impedances with the equations developed in the previous section, and in particular by substituting  $a_1, a_2, \epsilon$  and frequency in eq. (9). The required surface impedances of the covering metasurfaces in order to achieve scattering properties of the cylinders with twice and half radii are obtained as  $Z_s = -j517\Omega$  and  $Z_s = j761\Omega$ , respectively. We chose the parameters of the graphene nanopatches as  $D = 3.365 \mu\text{m}$ ,  $g = 0.59 \mu\text{m}$ ,  $T = 300 \text{ K}$  and  $\tau = 1.5 \text{ ps}$ . The optimized chemical potentials of the graphene to achieve the desired goals of case  $d_1$  ( $a_1 = 14 \mu\text{m}$ ) and case  $d_2$  ( $a_1 = 3.5 \mu\text{m}$ ), are  $0.66 \text{ eV}$  and  $0.14 \text{ eV}$ , respectively.

To prove the efficiency of the developed technique also for the case of conducting objects, in the following, we propose to transform the scattering properties of given conducting cylinder with the radius of  $a_2 = 9 \mu\text{m}$  to the ones of the target conducting cylinders with the radii of  $a_1 = 18 \mu\text{m}$  (case  $m_1$ ) and  $a_1 = 4.5 \mu\text{m}$ , (case  $m_2$ ) at  $f = 3 \text{ THz}$ . The dielectric layer, covering the given cylinder has relative permittivity  $\epsilon = 2$ , with the radius of  $a_c = 16 \mu\text{m}$ . Using eq. (14), the required surface impedances of the metasurfaces in order to make the object as if it has twice and half radii are obtained as  $Z_s = -j180 \Omega$  and  $Z_s = -j185 \Omega$ , respectively.  $D = 11.17 \mu\text{m}$ ,  $g = 2.5 \mu\text{m}$ ,  $T = 300 \text{ K}$  and  $\tau = 1.9 \text{ ps}$  are the parameters of the considered graphene nanopatches.

TABLE 1. Summary of the parameters of the designed metasurfaces.

		$\mu_c(\text{eV})$	$D(\mu\text{m})$	$g(\mu\text{m})$	$T(\text{K})$	$\tau(\text{ps})$
Dielectric	Case $d_1$	0.66	3.365	0.59	300	1.5
	Case $d_2$	0.14				
Metallic	Case $m_1$	0.64	11.17	2.5	300	1.9
	Case $m_2$	0.78				

To achieve the desired goals, the optimized chemical potentials are obtained as  $0.64 \text{ eV}$  and  $0.78 \text{ eV}$  for case  $m_1$  ( $a_1 = 18 \mu\text{m}$ ) and case  $m_2$  ( $a_1 = 4.5 \mu\text{m}$ ). Table 1 summaries the parameters of the designed metasurfaces for both cases, i.e., dielectric and conductive cores.

#### IV. RESULTS AND DISCUSSIONS

Here, we investigate the total scattering width (SW) of the given, coated and target cylinders to show that the desired scattering properties of the cylinders are obtainable by considering nanostructured graphene metasurfaces on them. Total SW is defined as follows [39]:

$$\text{Total SW} = \frac{4}{\beta_0} \sum_{n=-\infty}^{\infty} |C_n|^2 \quad (21)$$

where  $\beta_0$  is the propagation constant in free space, and  $c_n$ , is the  $n^{\text{th}}$  scattering coefficient.

Figures 3 and 4 show the total SW of the given, coated and target dielectric cylinders for case  $d_1$  (making the radius appears twice) and case  $d_2$  (making the radius appears half), respectively. We can see that at the operating frequency of 3 THz, total SW of the coated cylinder becomes equal to the total SW of the target cylinder, therefore the desired goal is achieved. Also the analytical results are validated with CST Microwave Studio [40], showing good agreement.

Figures 5 and 6 illustrate the electric field distribution for the corresponding cylinders in the both cases. By comparing Fig. 5(b) to 5(c) and Fig. 6(b) to 6(c) representing target and covered cylinders for the case  $d_1$  and  $d_2$ , it is understood that with covering the given cylinder by the designed metasurfaces, the electric field surrounding them as a result of TMz polarization plane wave illumination is transformed to the desired ones.

Figure 7 shows the RCS of the cylinders for cuts in the  $\phi = 90^\circ$  and for  $\theta = 90^\circ$  planes in polar coordinate system. They have been calculated using CST Microwave Studio, at the operating frequency and for both cases. It can be seen that although we focused on making the total SW of the target

$$c'_n = \frac{(J_n(\beta a_c) - \frac{J_n(\beta a_2)}{Y_n(\beta a_2)} Y_n(\beta a_c)) (\frac{Z_s}{j\eta_0} J'_n(\beta_0 a_c) - J_n(\beta_0 a_c)) - \frac{Z_s}{j\eta} J_n(\beta_0 a_c) (J'_n(\beta a_c) - \frac{J_n(\beta a_2) Y'_n(\beta a_c)}{Y_n(\beta a_2)})}{(J_n(\beta a_c) - \frac{J_n(\beta a_2)}{Y_n(\beta a_2)} Y_n(\beta a_c)) (H_n^{(2)}(\beta_0 a_c) - \frac{Z_s}{j\eta_0} H_n^{(2)'}(\beta_0 a_c)) + \frac{Z_s}{j\eta} H_n^{(2)}(\beta_0 a_c) (J'_n(\beta a_c) - \frac{J_n(\beta a_2) Y'_n(\beta a_c)}{Y_n(\beta a_2)})} \quad (14)$$

$$c'_0 = \frac{\pi \omega \mu a_c [Z_s \beta_0 a_c (\ln(\beta a_c) + \ln(\beta a_c)(\epsilon - 1))] + 2\eta_0 \pi Z_s}{4j\eta_0 Z_s \ln(\beta a_2) + \ln(\beta a_2) \ln(\beta a_c) \omega \mu a_c [4\eta_0 + 2j\epsilon Z_s \beta_0 a_c] - 4\eta_0 \omega \mu a_c \ln(\beta_0 a_c) \ln(\beta a_c)} \quad (15)$$

$$Z_s = j \frac{2\eta_0 \omega \mu a_c \ln(\frac{a_c}{a_2}) [-2 \ln(\beta_0 a_c) + M]}{-\omega \mu a_c \beta_0 a_c [M \ln(\beta a_c) + \ln(\beta a_2)(\epsilon - 1)] - 2\epsilon \ln(\beta a_2) \ln(\beta_0 a_c) + 2\eta_0 (2 \ln(\beta a_2) - M)} \quad (17)$$

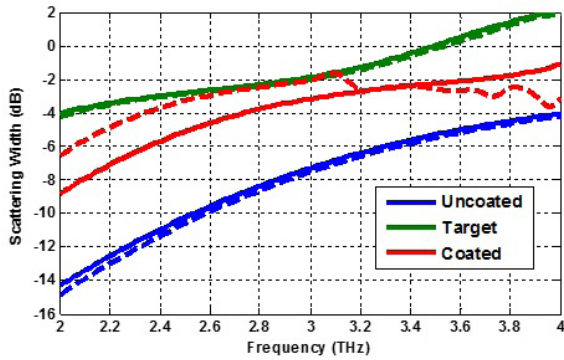


FIGURE 3. Total scattering width of the given, coated and target dielectric cylinders for the case  $d_1$ . Solid line: Analytical, Dashed line: Numerical.

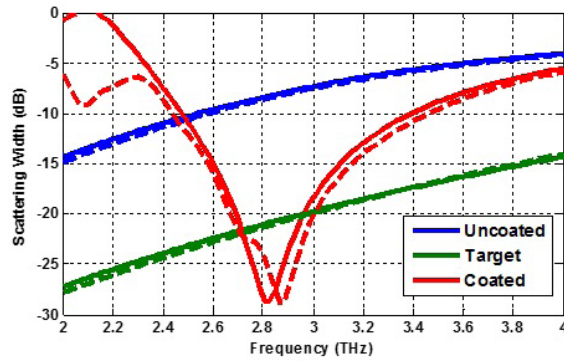


FIGURE 4. Total scattering width of the given, coated and target dielectric cylinders for the case  $d_2$ . Solid line: Analytical, Dashed line: Numerical.

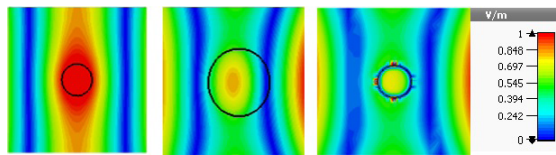


FIGURE 5. Amplitude distribution of electric field surrounding the a) given, b) target and c) coated dielectric cylinders for the case  $d_1$ .

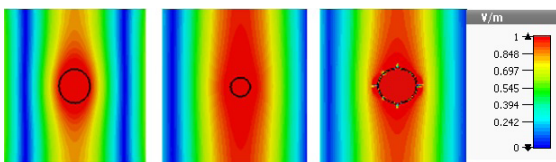


FIGURE 6. Amplitude distribution of electric field surrounding the a) given, b) target and c) coated dielectric cylinders for the case  $d_2$ .

and coated cylinders equal their 3D RCS in all observing angles of  $\phi$  and  $\theta$ , they have become almost the same, which shows that the designed metasurface performs as expected.

Figures 8 and 9 show the total SW of the given, coated and target conducting cylinders for the goals of case  $m_1$  (making the radius appears twice) and case  $m_2$  (making the radius appears half), respectively. The total SW of the coated cylinder becomes equal to the SW of that of the target cylinder at the center frequency of 3 THz, showing anticipated operation of the designed metasurface.

Figure 12 shows 3D RCS of the cylinders for  $\phi = 0^\circ$  and  $\theta = 90^\circ$  in polar coordinate system at the center frequency and for both cases. It can be understood that 3D RCS of the

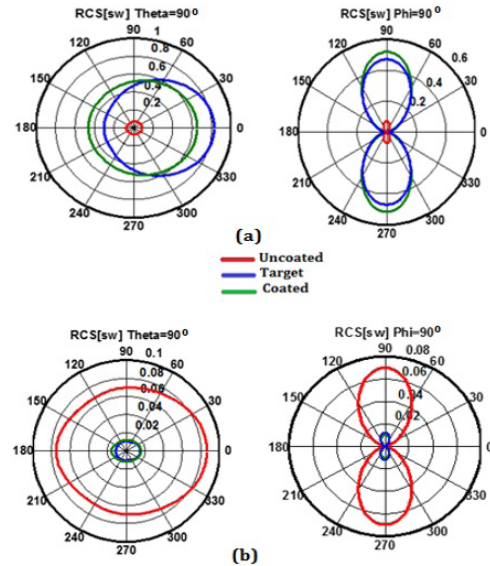


FIGURE 7. Polar RCS patterns of dielectric cylinders for  $\theta = 90^\circ$  and  $\phi = 90^\circ$  at 3 THz for a) case  $d_1$  and b) case  $d_2$ .

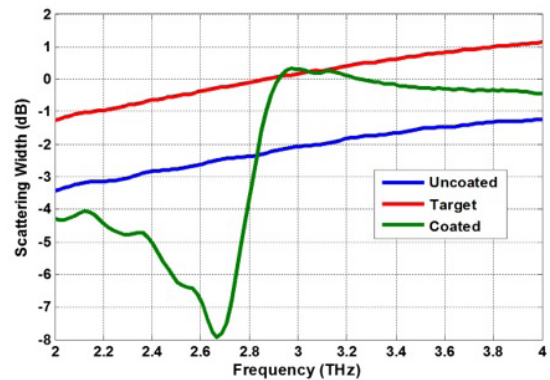


FIGURE 8. Numerical result for total scattering width of the given, coated and target conducting cylinders for the case  $m_1$ .

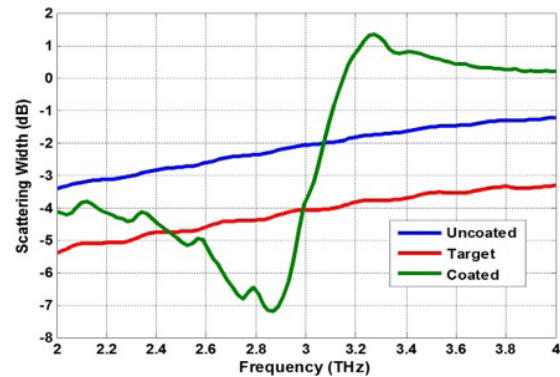


FIGURE 9. Numerical result for total scattering width of the given, coated and target conducting cylinders for the case  $m_2$ .

target and coated cylinders are almost equal for all observing angles.

Electric field distributions resulting from the perturbation of the impinging wave by the presented cylinders for the considered cases are shown in Figs. 10 and 11, which verify

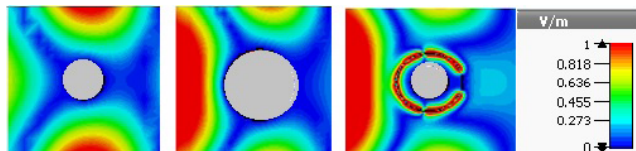


FIGURE 10. Amplitude distribution of electric field surrounding the a) given, b) target and c) coated conducting cylinders for the case  $m_1$ .

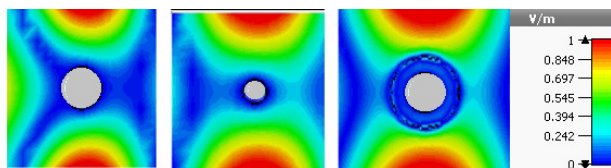


FIGURE 11. Amplitude distribution of electric field surrounding the a) given, b) target and c) coated conducting cylinders for the case  $m_2$ .

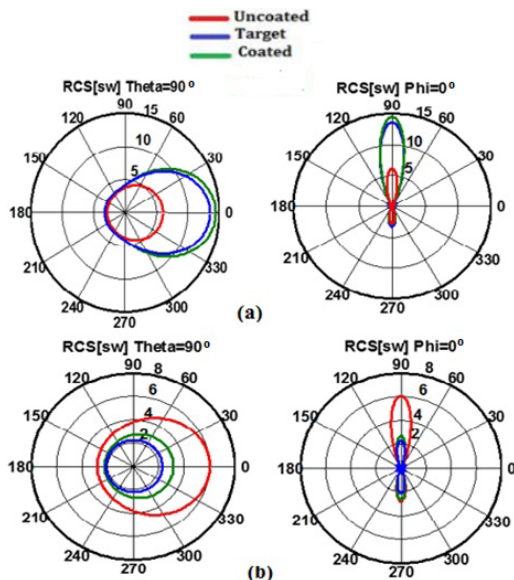


FIGURE 12. Polar RCS patterns of conducting cylinders for  $\theta = 90^\circ$  and  $\phi = 90^\circ$  at 3THz for a) case  $m_1$  and b) case  $m_2$ .

good similarity in field distributions for the target and coated cylinders.

## V. CONCLUSION

In this paper, we have analytically derived the required surface impedances of nanostructured graphene metasurfaces in order to achieve scattering manipulation of both dielectric and conducting cylinders. By changing the chemical potential of the graphene, its surface impedance can be adjusted to control the scattering properties of the given cylinders, without changing the geometry of the metasurfaces. From the results obtained analytically and confirmed numerically it can be concluded that the desired goals have been achieved and the coated cylinders can controllably scatter electromagnetic illumination corresponding to cylinders with different desired radii.

## REFERENCES

- [1] J. B. Pendry, "Controlling light on the nanoscale (Invited Review)," *Prog. Electromagn. Res.*, vol. 147, pp. 117–126, Jan. 2014.
- [2] A. K. Osanova, G. Labate, L. Matekovits, and A. A. Basharin, "Multipolar passive cloaking by nonradiating anapole excitation," *Sci. Rep.*, vol. 8, no. 1, Dec. 2018, Art. no. 12514.

- [3] G. Labate and L. Matekovits, "Invisibility and cloaking structures as weak or strong solutions of Devaney–Wolf theorem," *Opt. Express*, vol. 24, no. 17, p. 19245, Aug. 2016.
- [4] H. Chen, C. T. Chan, and P. Sheng, "Transformation optics and metamaterials," *Nature Mater.*, vol. 9, no. 5, pp. 387–396, May 2010.
- [5] J. Li and J. B. Pendry, "Hiding under the carpet: A new strategy for cloaking," *Phys. Rev. Lett.*, vol. 101, p. 203901, Nov. 2008.
- [6] D. Schurig et al., "Metamaterial electromagnetic cloak at microwave frequencies," *Science*, vol. 314, no. 5801, pp. 977–980, Oct. 2006.
- [7] U. Leonhardt, "Optical conformal mapping," *Science*, vol. 312, no. 5781, pp. 1777–1780, 2006.
- [8] J. B. Pendry, D. Schurig, and D. R. Smith, "Controlling electromagnetic fields," *Science*, vol. 312, pp. 1780–1782, Jun. 2006.
- [9] R. Liu, C. Ji, J. J. Mock, J. Y. Chin, T. J. Cui, and D. R. Smith, "Broadband ground-plane cloak," *Science*, vol. 323, no. 5912, pp. 366–369, Jan. 2009.
- [10] Z. Ruan, M. Yan, C. W. Neff, and M. Qiu, "Ideal cylindrical cloak: Perfect but sensitive to tiny perturbations," *Phys. Rev. Lett.*, vol. 99, no. 11, p. 113903, Sep. 2007.
- [11] F. Bilotti, S. Tricarico, and L. Vegni, "Plasmonic metamaterial cloaking at optical frequencies," *IEEE Trans. Nanotechnol.*, vol. 9, no. 1, pp. 55–61, Jan. 2010.
- [12] A. Alù and N. Engheta, "Plasmonic and metamaterial cloaking: Physical mechanisms and potentials," *J. Opt. A, Pure Appl. Opt.*, vol. 10, no. 9, p. 093002, Sep. 2008.
- [13] A. Alù and N. Engheta, "Cloaking and transparency for collections of particles with metamaterial and plasmonic covers," *Opt. Express*, vol. 15, no. 12, pp. 7578–7590, Jun. 2007.
- [14] A. Alù, D. Rainwater, and A. Kerkhoff, "Plasmonic cloaking of cylinders: Finite length, oblique illumination and cross-polarization coupling," *New J. Phys.*, vol. 12, no. 10, p. 103028, Oct. 2010.
- [15] B. Edwards, A. Alù, M. Young, M. Silveirinha, and N. Engheta, "Experimental verification of epsilon-near-zero metamaterial coupling and energy squeezing using a microwave waveguide," *Phys. Rev. Lett.*, vol. 100, no. 3, p. 033903, Jan. 2008.
- [16] A. Alù and N. Engheta, "Achieving transparency with plasmonic and metamaterial coatings," *Phys. Rev. E, Stat. Phys. Plasmas Fluids Relat. Interdiscip. Top.*, vol. 72, no. 1, p. 016623, Jul. 2005.
- [17] G. Labate, A. Alù, and L. Matekovits, "Surface-admittance equivalence principle for nonradiating and cloaking problems," *Phys. Rev. A, Gen. Phys.*, vol. 95, no. 6, p. 063841, Jun. 2017.
- [18] E. Shokati, N. Granpayeh, and M. Danaeifar, "Wideband and multi-frequency infrared cloaking of spherical objects by using the graphene-based metasurface," *Appl. Opt.*, vol. 56, no. 11, pp. 3053–3058, Apr. 2017.
- [19] M. Danaeifar and N. Granpayeh, "Wideband invisibility by using inhomogeneous metasurfaces of graphene nanodisks in the infrared regime," *J. Opt. Soc. Amer. B, Opt. Phys.*, vol. 33, no. 8, pp. 1764–1768, Aug. 2016.
- [20] A. Monti, J. C. Soric, A. Alù, A. Toscano, and F. Bilotti, "Anisotropic mantle cloaks for TM and TE scattering reduction," *IEEE Trans. Antennas Propag.*, vol. 63, no. 4, pp. 1775–1788, Apr. 2015.
- [21] Y. R. Padooru, A. B. Yakovlev, P.-Y. Chen, and A. Alù, "Analytical modeling of conformal mantle cloaks for cylindrical objects using sub-wavelength printed and slotted arrays," *J. Appl. Phys.*, vol. 112, no. 3, p. 034907, 2012.
- [22] P.-Y. Chen and A. Alù, "Mantle cloaking using thin patterned metasurfaces," *Phys. Rev. B, Condens. Matter*, vol. 84, no. 20, p. 205110, Nov. 2011.
- [23] A. Alù, "Mantle cloak: Invisibility induced by a surface," *Phys. Rev. B, Condens. Matter*, vol. 80, no. 24, p. 245115, Dec. 2009.
- [24] L. Matekovits and T. S. Bird, "Width-modulated microstrip-line based mantle cloaks for thin single- and multiple cylinders," *IEEE Trans. Antennas Propag.*, vol. 62, no. 5, pp. 2606–2615, May 2014.
- [25] Z. Hamzavi-Zarghani, A. Yahaghi, and A. Bordbar, "Analytical design of nanostructured graphene metasurface for controllable scattering manipulation of dielectric cylinder," in *Proc. 26th Iranian Conf. Elect. Eng. (ICEE)*, 2018, pp. 592–595.
- [26] S. Vellucci, A. Monti, A. Toscano, and F. Bilotti, "Scattering manipulation and camouflage of electrically small objects through metasurfaces," *Phys. Rev. Appl.*, vol. 7, no. 3, p. 034032, Mar. 2017.
- [27] A. Farmani, M. Yavarian, A. Alighanbari, M. Miri, and M. H. Sheikhi, "Tunable graphene plasmonic Y-branch switch in the terahertz region using hexagonal boron nitride with electric and magnetic biasing," *Appl. Opt.*, vol. 56, no. 32, pp. 8931–8940, Nov. 2017.

- [28] M. Yarahmadi, M. K. Moravvej-Farshi, and L. Yousefi, "Subwavelength graphene-based plasmonic THz switches and logic gates," *IEEE Trans. THz Sci. Technol.*, vol. 5, no. 5, pp. 725–731, Sep. 2015.
- [29] A. Farmani, M. Miri, and M. H. Sheikhi, "Design of a high extinction ratio tunable graphene on white graphene polarizer," *IEEE Photon. Technol. Lett.*, vol. 30, no. 2, pp. 153–156, Jan. 15, 2018.
- [30] Z. Hamzavi-Zarghani, A. Yahaghi, and L. Matekovits, "Reconfigurable metasurface lens based on graphene split ring resonators using Pancharatnam–Berry phase manipulation," *J. Electromagn. Waves Appl.*, Jan. 2019. [Online]. Available: <https://www.tandfonline.com/doi/full/10.1080/09205071.2018.1563509>, doi: 10.1080/09205071.2018.1563509.
- [31] C. Wang et al., "Dynamically tunable deep subwavelength high-order anomalous reflection using graphene metasurfaces," *Adv. Opt. Mater.*, vol. 6, no. 3, p. 1701047, Feb. 2018.
- [32] Z. Li, W. Liu, H. Cheng, S. Chen, and J. Tian, "Tunable dual-band asymmetric transmission for circularly polarized waves with graphene planar chiral metasurfaces," *Opt. Lett.*, vol. 41, no. 13, pp. 3142–3145, Jul. 2016.
- [33] J. Li et al., "Optical polarization encoding using graphene-loaded plasmonic metasurfaces," *Adv. Opt. Mater.*, vol. 4, no. 1, pp. 91–98, Jan. 2016.
- [34] W. Tang, L. Wang, X. Chen, C. Liu, A. Yu, and W. Lu, "Dynamic metamaterial based on the graphene split ring high-Q fano-resonator for sensing applications," *Nanosci.*, vol. 8, no. 33, pp. 15196–15204, 2016.
- [35] E. S. Torabi, A. Fallahi, and A. Yahaghi, "Evolutionary optimization of graphene-metal metasurfaces for tunable broadband terahertz absorption," *IEEE Trans. Antennas Propag.*, vol. 65, no. 3, pp. 1464–1467, Mar. 2017.
- [36] Z. Hamzavi-Zarghani, A. Yahaghi, L. Matekovits, and I. Peter, "Tunable polarization converter based on graphene metasurfaces," *Proc. IEEE Radio Conf.*, Oct. 2018, pp. 1–2.
- [37] P.-Y. Chen, J. Soric, Y. R. Padooru, H. M. Bernety, A. B. Yakovlev, and A. Alù, "Nanostructured graphene metasurface for tunable terahertz cloaking," *New J. Phys.*, vol. 15, pp. 123029–1–123029–12, Dec. 2013.
- [38] Y. R. Padooru, A. B. Yakovlev, C. S. R. Kaipa, G. W. Hanson, F. Medina, and F. Mesa, "Dual capacitive-inductive nature of periodic graphene patches: Transmission characteristics at low-terahertz frequencies," *Phys. Rev. B, Condens. Matter*, vol. 87, no. 11, p. 115401, Mar. 2013.
- [39] C. A. Balanis, *Advanced Engineering Electromagnetics*, 3rd ed. New York, NY, USA: Wiley, 1989.
- [40] G. Labate, S. K. Podilchak, and L. Matekovits, "Closed-form harmonic contrast control with surface impedance coatings for conductive objects," *Appl. Opt.*, vol. 56, no. 36, pp. 10055–10059, Dec. 2017.
- [41] J. C. Soric, P. Y. Chen, A. Kerkhoff, D. Rainwater, K. Melin, and A. Alù, "Demonstration of an ultralow profile cloak for scattering suppression of a finite-length rod in free space," *New J. Phys.*, vol. 15, no. 3, p. 033037, 2013.
- [42] A. Forouzmmand and A. B. Yakovlev, "Electromagnetic cloaking of a finite conducting wedge with a nanostructured graphene metasurface," *IEEE Trans. Antennas Propag.*, vol. 63, no. 5, pp. 2191–2202, May 2015.
- [43] V. P. Gusynin, S. G. Sharapov, and J. P. Carbotte, "On the universal ac optical background in graphene," *New J. Phys.*, vol. 11, no. 9, p. 095013, Sep. 2009.
- [44] G. W. Hanson, "Dyadic Green's functions and guided surface waves for a surface conductivity model of graphene," *J. Appl. Phys.*, vol. 103, no. 6, pp. 064302–1–064302–8, Mar. 2008.
- [45] C. F. Bohren and D. R. Huffman, Eds., *Absorption and Scattering of Light by Small Particles*. Weinheim, Germany: Wiley, 1998.
- [46] *CST Microwave Studio*, Comput. Simul. Technol. AG, 2018.



**ALIREZA YAHAGHI** received the B.S. degree in electrical engineering from the University of Tehran, Tehran, Iran, in 2002, the M.Sc. degree in fields and waves communication engineering from the Iran University of Science and Technology, Tehran, in 2004, and the Ph.D. degree from Shiraz University, Shiraz, Iran, in 2010, where he is currently a full-time Assistant Professor with the Department of Communication and Electronics Engineering. From 2008 to 2009, he was with

the Laboratory for Electromagnetic Fields and Microwave Electronics (IFH), ETH Zürich, Zürich, Switzerland, as an Academic Guest. From 2014 to 2016, he was an Alexander von Humboldt Researcher with the Ultrafast Optics and X-Rays Division, CFEL, DESY, Hamburg, Germany. His research interests include numerical methods in electromagnetics and optics, metamaterials and metasurfaces, plasmonics, and transformation optics.



**LADISLAU MATEKOVITS** (M'94–SM'11) received the degree in electronic engineering from the Politehnica University of Bucharest, Bucharest, Romania, in 1992, and the Ph.D. degree (Dottorato di Ricerca) in electronic engineering from the Politecnico di Torino, Turin, Italy, in 1995. Since 1995, he has been with the Department of Electronics and Telecommunications, Politecnico di Torino, first as a Postdoctoral Fellow and then as a Research Assistant, where he became an Assistant Professor, in 2002, and was appointed as a Senior Assistant Professor, in 2005, and as an Associate Professor, in 2014. In 2017, he obtained the Full Professor qualification in Italy. In 2005, he was a Visiting Scientist with the Antennas and Scattering Department, Fraunhofer Institute, Wachtberg, Germany. From 2009 to 2011, he has been a Marie Curie Fellow with Macquarie University, Sydney, NSW, Australia, where, in 2013, he also held a visiting academic position and, in 2014, was appointed as an Honorary Fellow.

His main research activities concern numerical analysis of printed antennas and, in particular, the development of new, numerically efficient full-wave techniques to analyze large arrays, optimization techniques, and active and passive metamaterials for cloaking applications. Material parameter retrieval of these structures by inverse methods and different optimization techniques has also been considered. In the last years, bio-electromagnetic aspects have also been contemplated, as, for example, the design of implantable antennas or the development of nano-antennas, for example, for drug delivery applications.

He has published more than 300 papers, including more than 65 journal contributions, and has delivered seminars on these topics all around the world: Europe, USA (AFRL/MIT-Boston), Australia, China, and Russia. He has been invited to serve as a Research Grant Assessor for government funding calls (Romania, Italy, and Croatia) and as an International Expert in Ph.D. thesis evaluation by several Universities from Australia, India, Pakistan, and Spain.

Dr. Matekovits was a recipient of various awards in international conferences, including the 1998 URSI Young Scientist Award in Thessaloniki, Greece, the Barzilay Award 1998 (Young Scientist Award, granted every two years by the Italian National Electromagnetic Group), and the Best AP2000 Oral Paper on Antennas, ESA-EUREL Millennium Conference on Antennas and Propagation in Davos, Switzerland.

Since 2010, he has been a member of the Organizing Committee of the International Conference on Electromagnetics in Advanced Applications. He is a member of the technical program committees of several conferences. He has been the Assistant Chairman and the Publication Chairman of the European Microwave Week 2002 in Milan, Italy, and the General Chair of the 11th International Conference on Body Area Networks (BodyNets) 2016. He serves as an Associate Editor for the IEEE ACCESS, the IEEE ANTENNAS AND WIRELESS PROPAGATION LETTERS, and IET MAP and a Reviewer for different journals.



**ZAHRA HAMZAVI-ZARGHANI** was born in Shiraz, Iran. She received the B.Sc. degree in electrical engineering from Shiraz University, Shiraz, in 2010, and the M.Sc. degree in electrical engineering from Tarbiat Modares University, Tehran, Iran, in 2014. She is currently pursuing the joint Ph.D. degree in electrical engineering with Shiraz University and the Politecnico di Torino, Turin, Italy. Her research interests include metamaterial and metasurfaces, imaging, scattering manipula-

tion and cloaking, transmitarray and reflectarray antennas, graphene, and tunable applications.